Published in final edited form as:
Biomaterials. 2014 March ; 35(8): 2507–2517. doi:10.1016/j.biomaterials.2013.12.009.

Tunable Staged Release of Therapeutics from Layer-by-Layer Coatings with Clay Interlayer Barrier

Jouha Min[1,2], **Richard D. Braatz**[1], and **Paula T. Hammond**[1,2,*]

[1]Department of Chemical Engineering, Massachusetts Institute of Technology, Cambridge, MA 02139, USA

[2]David H. Koch Institute for Integrative Cancer Research, Cambridge, MA 02139, USA

Abstract

In developing new generations of coatings for medical devices and tissue engineering scaffolds, there is a need for thin coatings that provide controlled sequential release of multiple therapeutics while providing a tunable approach to time dependence and the potential for sequential or staged release. Herein, we demonstrate the ability to develop a self-assembled, polymer-based conformal coating, built by using a water-based layer-by-layer (LbL) approach, as a *dual-purpose* biomimetic implant surface that provides staggered and/or sustained release of an antibiotic followed by active growth factor for orthopedic implant applications. This multilayered coating consists of two parts: a base osteoinductive component containing bone morphogenetic protein-2 (rhBMP-2) beneath an antibacterial component containing gentamicin (GS). For the fabrication of truly stratified composite films with the customized release behavior, we present a new strategy—implementation of laponite clay barriers—that allows for a physical separation of the two components by controlling interlayer diffusion. The clay barriers in a single-component GS system effectively block diffusion-based release, leading to approximately 50% reduction in bolus doses and 10-fold increase in the release timescale. In a *dual-therapeutic* composite coating, the top GS component itself was found to be an effective physical barrier for the underlying rhBMP-2, leading to an order of magnitude increase in the release timescale compared to the single-component rhBMP-2 system. The introduction of a laponite interlayer barrier further enhanced the temporal separation between release of the two drugs, resulting in a more physiologically appropriate dosing of rhBMP-2. Both therapeutics released from the composite coating retained their efficacy over their established release timeframes. This new platform for multi-drug localized delivery can be easily fabricated, tuned, and translated to a variety of implant applications where control over spatial and temporal release profiles of multiple drugs is desired.

Keywords

Controlled drug release; BMP (bone morphogenetic protein); Antibacterial; Bone; Silicate; Layer-by-Layer; Coating

*To whom correspondence should be addressed: **Paula T. Hammond**, Postal Address: 77 Massachusetts Avenue, Cambridge, MA 02139, USA, Telephone: 617-253-3016, Fax: 617-253-8757, hammond@mit.edu.

Conflict of Interest

The authors confirm that there are no known conflicts of interest associated with this publication.

1. Introduction

Recently, the concept of generating multi-component delivery systems that provide localized release of multiple therapeutics over appropriate timescales and with precise doses has been of great interest for many drug delivery and tissue engineering applications [1–3]. In particular, there is a need for a multi-agent delivery thin film platform that can conformally coat complex implant, scaffold and device surfaces and release a range of different kinds of drugs, with independent control of order, timing, and rate of release. Despite the promise of multi-component delivery, the ability to generate a multi-component system with highly tailored release profiles has remained a challenge due to the lack of materials and methods that enable incorporation of a range of sensitive biologic drugs while preserving their activity *and* provide spatial and temporal control over the release of the therapeutics. The layer-by-layer assembly (LbL) technique—a method involving the alternate adsorption of oppositely charged polymers—is one of the most suitable methods for generating multi-component coatings due to its simplicity, ease of application, and water-based assembly [4]. Its conformal nature provides the flexibility to incorporate a broad range of biomaterials, including those with nonplanar complex geometries and large surface area such as microneedles [5] and nanoparticles [6, 7]. LbL assembly holds significant promise in the ability to easily tune the loading of materials and control the order and location of multiple layers with nano-scale precision [1, 8], and this promise is furthered by recent demonstrations that LbL films provide controlled and tunable release of therapeutics from surfaces [9–11].

A rapidly expanding area in regenerative medicine and tissue engineering is the development of biomimetic surface coatings on orthopedic implants that can accelerate the bone healing process while preventing infection. Millions of orthopedic implants are performed annually, with bone implant integration being a common clinical issue. However, due to surgical and implant-related complications, approximately 12% of patients have to receive revision replacements within 10 years after surgery [12]. Among the primary reasons for joint failure, implant-related infections create complications for patients and cost close to $2 billion in annual treatment. For this reason, prevention or elimination of infection following a revision operation is key for successful patient recovery. Today's gold standard for treatment of implant-associated infection is two-stage re-implantation, which involves six weeks of antibiotic therapy before introduction of the new implant, and two surgeries. Although relatively effective at eradicating infection, this treatment method has several drawbacks including long periods of hospitalization, morbidity, requirement of a second surgery for removal of the antibiotic beads or spacer, and sometimes increased mortality [13]. Therefore, there is a strong need for a single-stage re-implantation such as a drug-device combination system, which can treat bacterial infection as new bone is generated at the interface of the implant. Recent studies have demonstrated that co-administration of an antibiotic and a growth factor has potential beneficial effects and thus results in more favorable clinical outcomes such as increased bone formation, compared to single administration of the individual antibiotic and growth factor controls [14, 15]. A dual-purpose system with customized release behavior can reduce the incidence of implant failure due to post-operative infection and mechanical loosening *in situ* [14, 16].

In previous work, we have demonstrated that antibiotics can be released from LbL coated implant surfaces to address infection in a rabbit model [17]; furthermore, we have independently shown the power of single and dual growth factor LbL films to modulate the integration of bone on implant surfaces, and to yield dense and highly vascularized bone in 3D scaffolds in rats [18–21]. Given the advantages of multi-component delivery and the LbL assembly technique, attempting to develop a multi-agent LbL film is a natural next step. Recent efforts have been directed at developing truly stratified LbL films, but

unfortunately, many such approaches have been unsuccessful because of interlayer diffusion, a phenomenon that leads to mixing and sometimes exchange of film components during assembly [22, 23]. To block interlayer diffusion in the LbL films, we and other groups have investigated a range of methods and materials including polymer barrier layers [24–27] and graphene oxide [9]. Despite the many promising achievements, the aforementioned approaches still present some limitations for certain drug delivery and tissue engineering applications; some covalent chemistries are incompatible with biologic drugs, and newer nanomaterial components such as graphene oxide [28] are still under investigation with regard to their safety as biomaterials.

Laponite clay, a disk-shaped synthetic silicate $Na^{+}_{0.7}[Si_8Mg_{5.5}Li_{0.3}H_4O_{24}]^{-}_{0.7}$ with dimensions of 25 nm in diameter and 0.92 nm in thickness, is readily available, low-cost and is generally regarded as safe (GRAS) by the FDA as a natural clay product; the nanomaterial also exhibits some favorable bioactive properties [29]. Recent studies have demonstrated that laponite can induce osteogenic differentiation of stem cells and develop microenvironments that support tissue regeneration [30, 31]. In the area of drug delivery, laponite nanoplatelets have been utilized to modulate release properties because of their intercalation capacity [32–35]. Also, laponite and montmorillonite clays have been used in varying amounts as components of LbL films to enhance their mechanical properties by increasing modulus and durability [36, 37]. To this end, laponite clay was considered as a most appropriate two-dimensional barrier material that can physically block interlayer diffusion and sustain release of loaded drugs.

In this study, the primary goal was to develop a multi-agent delivery thin film LbL platform with controlled local release of an antibiotic, gentamicin sulfate, and an osteoinductive growth factor, rhBMP-2, in a manner that is biologically relevant and leads to increased efficacy. Orthopedic implant surfaces modified using this multi-drug LbL coating can fulfill the need for controlled delivery of multiple therapeutic agents for healing bone defects, inducing osteointegration on the implant surface while preventing infection at the implant site. A suitable multi-drug delivery platform would exhibit a rapid release of an antibiotic for the first few days, followed by a sustained release for multiple weeks along with a controlled release of a growth factor. In this article, we fabricated a series combination of an rhBMP-2 film component and a GS component in multilayer films with and without laponite barrier layers with the aim of demonstrating the laponite clay barrier interlayer as an effective means of modulating release. We hypothesize that such an approach can provide a means to achieve this kind of customized delivery behavior, with staggered release of antibiotic followed by active growth factor. To evaluate the bioactivity of the films, the efficacy of both components over their established release timeframes was assessed *in vitro*.

2. Materials and Methods

2.1 Materials

Poly(β-amino esters), Poly1 (M_n ~ 10 kDa) and Poly2 (M_n ~ 11 kDa), were synthesized as previously described [38]. Poly(acrylic acid) (PAA, M_w ~ 450 kDa and 1.25 MDa), Chitosan (Chi, M_v ~ 110–150 kDa) poly(diallyldimethylammonium chloride) (PDAC, M_w ~ 200–300 kDa), 3 M sodium acetate buffer (NaOAc, pH 5.2), as well as solvents and common buffers, were purchased from Sigma-Aldrich (St. Louis, MO). Laponite was purchased from Southern Clay Products (Gonzales, TX). Recombinant human BMP-2 (rhBMP-2) was a gift from Pfizer Inc. (Cambridge, MA). Non-radiolabeled gentamicin sulfate (GS) was purchased from Mediatech, Inc. (Herndon, VA), and radiolabeled gentamicin ^{3}H-GS (250 μCi total, 1 mCi/mL in ethanol, 200 μCi/mg) was purchased from American Radiolabeled Chemicals (St. Louis, MO). Silicon wafers were purchased from Silicon Quest International

(Santa Clara, CA). All materials and solvents were used as received without further purification.

S. aureus UAMS-1 (ATCC 49230) and MC3T3-E1 subclone 4, a mouse preosteoblasts cell, were purchased from ATCC (Manassas, VA). Cation-adjusted Mueller Hinton broth (CaMHB), Bacto agar, and gentamicin standard disks were purchased from BD Biosciences (San Jose, CA). Alpha minimum essential medium (α-MEM), fetal bovine serum (FBS), trypsin-EDTA, and phosphorate buffered saline (PBS) were purchased from Invitrogen (Carlsbad, CA).

2.2 Preparation of polyelectrolyte solutions

For GS component, dipping solutions of poly1 and PAA (M_w ~ 1.25 MDa) were prepared at 2 mg/mL in 100 mM sodium acetate buffer and pH adjusted to 5.0. The dipping solution of GS was at 10 mg/mL in 100 mM sodium acetate buffer. For *in vitro* release studies, a small amount of ^{3}H-GS was added to the 10 mg/mL GS solution to yield the end product of 0.5 μCi/mL; the molar ratio of ^{3}H-GS to regular GS was 1/4000. For the rhBMP-2 component, dipping solutions of poly2 and PAA (M_w ~ 450 kDa) were prepared at 1 mg/mL in 100 mM sodium acetate buffer and pH adjusted to 4.0. The dipping solution of rhBMP-2 was at 40 μg/mL in 100 mM sodium acetate buffer.

2.3 Layer-by-layer film formation

Silicon substrates with dimensions of 0.5 × 2.0 cm^2 were used for all *in vitro* experiments. In all cases, substrates were rinsed with methanol and ultra-pure water, dried under nitrogen, and plasma etched in oxygen at high RF power for 90 sec using a Harrick PDC-32G plasma cleaner. The cleaned silicon substrates were immediately immersed in the first cationic solution. First, tetralayer films were fabricated at room temperature using an automated dipping robot (Carl Zeiss HMS Series Programmable Slide Stainer) by alternate dipping in a solution of cationic species for 5 min followed by two consecutive rinse steps in 100 mM sodium acetate baths for 30 and 60 sec, and then into anionic species for 5 min followed by the same rinse cycle. The entire cycle was repeated until the desired number of tetralayers was deposited. Following the film deposition, the films were allowed to dry and then stored at 4 °C prior to subsequent analysis.

2.4 Deposition of polymer/clay barrier layers

The polymer/clay barrier layers were deposited in between and/or atop the tetralayer films using the spray-LbL technique. Solutions of Chitosan (0.2 mg/mL) or PDAC (2 mM) and Lap (0.1 wt%) were prepared in ultra-pure water and pH adjusted to 4 and 9, respectively. The bilayers were fabricated using a programmable spraying apparatus (Svaya Nanotechnologies) by alternate spraying a solution of cationic species for 1 sec at a flow rate of 0.4 mL/sec followed by drying step for 30–60 sec, and then a solution of anionic species for 1 sec followed by the same drying step. The entire cycle was repeated until the desired number of bilayers was deposited.

2.5 Film characterization

Film thickness and surface roughness were determined by Dektak Stylus profilometer (Veeco Instruments Inc.). Films in the dry state were scratched with a razor blade, and thickness was measured at three predetermined locations. Film cross-sections and surfaces were examined using a scanning electron microscope (JEOL JSM-6700F) and energy-dispersive x-ray spectroscopy (EDS). The surface morphology and roughness of the LbL films were observed using an atomic force microscope (Nanoscope IIIa; Digital Instruments) in tapping mode.

2.6 Release characterization

Films with protein (rhBMP-2) and antibiotic (GS + ^{3}H-GS) were immersed into 1 mL of phosphate buffer solution (PBS) with pH 7.4 in a capped 2-mL micro-centrifuge tube maintained at 37 °C. At predetermined time points, 0.5 mL of sample was collected from the tube and replaced with 0.5 mL of pre-warmed PBS. This process was performed in a gentle manner such that it does not cause any mechanical disturbance to the films. Samples were stored at –20 °C until analyzed. The samples from consecutive time points were then analyzed by bacterial and/or cellular assays (see below).

For rhBMP-2 quantification, an ELISA development kit (Peprotech Inc., Rocky Hill, NJ) was used. For GS, each 0.5 mL sample was then mixed with 5 mL of ScintiSafe Plus 50% (Fisher Scientific, Atlanta, GA) prior to the quantification. The mixtures are analyzed using a Tricarb Model 2810 TR liquid scintillation counter (Perkin Elmer, Waltham, MA). The raw data given in disintegrations per minute (DPM) is converted to the mass of GS by using a calibration curve of [concentration versus DPM], which is linear over the GS concentration range used in this study. The total cumulative GS released from the film at a given time point *i* can be calculated by

$$m_i = C_i V_i + (0.5\text{mL}) \sum_{j=1}^{i-1} C_j$$

where m_i (μg) is the total cumulative amount of GS released at time point (i), C_i (μg/mL) is the concentration of sample *i*, V_i (mL) is the total volume of the release medium, and the summation term adds up the total extensive quantity of GS removed in each of the previous aliquots.

2.7 S.aureus antimicrobial susceptibility assays

The efficacy of GS loaded on the LbL films was evaluated by exploring the activity of the LbL films directly as well as drug release solutions using the previously described methods [17]. Briefly, the LbL film activity was assessed directly using a Kirby-Bauer disk diffusion assay on a bacteria-coated agar plate. Agar plates were inoculated with exponentially growing *S.aureus* in cation-adjusted Mueller Hinton broth (CMHB) at 10^8 CFU/mL and incubated at 37 °C for 16–18 h. The diameter of inhibition zone was measured in millimeters.

A quantitative determination of GS activity from the LbL films was obtained according to a previously published microdilution procedure [39] in CMHB with an inoculation of 10^5 CFU/mL. The 96-well clear bottom plate was incubated at 37 °C for 16–18 h and read at 600 nm in a Tecan Infinite® 200 PRO microplate reader. Normalized bacteria inhibition was calculated using

$$\text{Normalized S. aureus density} = \frac{OD_{600,\text{sample}} - OD_{600,\text{negative control}}}{OD_{600,\text{positive control}} - OD_{600,\text{negative control}}}$$

2.8 Cell culture

To determine the efficacy of the release of growth factors from the LbL films and the cytotoxic effect of the films, *in vitro* tests were performed to quantify and visualize the effects on pre-osteoblast cell line MC3T3-E1 with high osteoblast differentiation and

mineralization activity. rhBMP-2 initiates the differentiation of pre-osteoblast MC3T3-E1 into bone.

MC3T3-E1 cells were cultured in growth medium (α-MEM supplemented with 10% FBS and 1% of antibiotic and antimycotic solution) in a humidified incubator (37 °C; 5% CO_2 in air). Growth medium was replenished every 2–3 days and cells were subcultured when near 100% confluence with the use of 0.05% trypsin-EDTA. All cells used in these studies were less than passage number 12.

Elution buffers were prepared by incubating each LbL film in 2 mL of growth medium at 37 °C. At predetermined time points, the release media was replaced with pre-warmed media. The extracted samples were stored at –20 °C until analyzed.

Cells were seeded at a density of 10^4 cells/cm^2 in the wells of 6-well or 12-well tissue culture plates (Corning) and incubated at 37 °C and 5% CO_2 in humidified air for 24–48 h prior to exposure to delivery platforms containing rhBMP-2 or elution buffers in cellular assays. Each delivery platform containing rhBMP-2 was placed on a culture insert (Transwell®, Corning) in the culture plate. The growth medium was changed to growth medium or differentiation medium (growth medium supplemented with 10 mM of β-glycerol phosphate and 50 mg/mL of L-ascorbic acid) and incubated with the plated MC3T3-E1 cells prior to evaluation.

2.9 Alkaline phosphatase activity assay

Alkaline phosphatase (ALP) activity was measured on day 6 after the initiation of MC3T3-E1 osteogenic differentiation using the Alkaline Phosphatase Colorimetric Assay kit (Abcam), which quantifies the ALP enzyme activity. The assay was performed according to the manufacturer's specifications. The ALP activity measurements were then normalized to total protein determined by BCA assay (Pierce). For colorimetric ALP detection, NBT (nitro-blue tetrazolium chloride) and BCIP (5-bromo-4-chloro-3'-indolyphosphate p-toluidine salt) substrate solution (Pierce) was incubated with cells for 20 min at 37 °C. Cells were then washed in DI water, and the stained cultures were visualized under phase contrast microscopy.

2.10 Alizarin red S differentiation assay

After 14–21 days of exposure to different formulations of the release medium, MC3T3-E1 cells were assayed for calcium deposition using Alizarin red S (ARS). Cells were washed with PBS and fixed with 4% paraformaldehyde for 10 min. After three rinses with DI water, ARS stain solution (2% ARS in DI water pH adjusted to 4.1 with 10% ammonium hydroxide) was incubated with cells for 20 min at room temperature. Cells were then washed in DI water 4 times for 2 min each. The ARS-stained cultures were visualized under phase contrast microscopy. The ARS stain was quantified using a previously published protocol [40]. The ARS-stained cultures were incubated in 10% acetic acid for 30 min at room temperature, and the cell layers were disrupted by the use of a pipette tip. The cell suspensions were transferred to a microcentrifuge tube, vortexed, and heated at 85 °C for 10 min. After transferring to ice for 5 min, the tubes were centrifuged at 16,000 g for 15 min and pH adjusted to pH 4.1–4.5. Triplicates with growth and differentiation medium controls were read on a 96-well plate with black sides and a clear bottom at 405 nm in a Tecan Infinite® 200 PRO microplate reader.

2.11 Cell viability assays

After 16–18 h of exposure to different formulations of the release medium, MC3T3-E1 cells were examined by the use of the CellTiter-Glo® Luminescent Cell Viability Assay

(Promega, Madison, WI) and the Live/Dead® Viability/Cytotoxicity Kit (Invitrogen, Carlsbad, CA). CellTiter-Glo® luminescent assay is a method to determine the cell viability based on quantitation of the ATP present, which signals the presence of metabolically active cells, and Live/Dead® Viability/Cytotoxicity assay is for determination of live and dead cell populations by fluorescent-confocal imaging. The viability assays were performed according to the manufacturer's specifications.

2.12 Statistical analysis

All data analysis was performed in GraphPad Prism 5 software (San Diego, CA). Data are reported as mean ± standard deviation of a minimum of 3 samples. Statistical significance ($P < 0.05$) was determined by GraphPad Prism 5 software using one-way ANOVA with a Tukey post hoc test.

3. Results and Discussion

3.1 Design of Combination Films with Dual Functionality

In this study, multi-component LbL films consisting of a base osteoinductive component containing bone morphogenetic protein-2 (rhBMP-2) beneath an antibacterial component containing gentamicin (GS) were fabricated with the purpose of demonstrating that these very different therapeutic molecules could both be delivered from the same platform film, and that the release characteristics could be tuned for treatment of infection *and* bone regeneration. Figure 1 contains the structures of the polyions, and the biologic and small molecule drug components incorporated into the LbL coatings for this study.

Both of the therapeutics selected for this system present unique delivery challenges and desired release quantities and time periods. rhBMP-2 is one of the proven osteoinductive growth factors that promote bone growth. Current systems for growth factor delivery exhibit bolus release upon implantation, which is generally unfavorable and suboptimal because of rapid clearance of the majority of the growth factor from the target site [20, 41]. The effects of rhBMP-2 are dose dependent, but quantities far above physiological levels can result in a lowered impact on tissue regeneration as well as undesired and often serious side effects such as cancer. The increased cost of production for such large amounts of factor also greatly limits the promise of commercial translation to clinic for such systems [41]. The antibiotic gentamicin sulfate (GS) is a water-soluble aminoglycoside with a minimum inhibitory concentration of 0.12–0.25 μg/mL against strains of *S. aureus* [42]. Because gentamicin at elevated systemic levels can cause adverse effects on osteoblast cell proliferation [43], localized delivery of gentamicin at low concentrations is advantageous. Under conditions of acidic and physiological pH, both rhBMP-2 and GS are expected to be positively charged and can therefore be incorporated into LbL films under slightly acidic deposition conditions.

A series combination of an rhBMP-2 film component and a GS component with and without the laponite barrier layers was fabricated and examined. For the rhBMP-2 component, a polycationic degradable poly(β-amino esters), Poly2, was alternated with anionic PAA and positively charged rhBMP-2 in the form of tetralayers, written as [Poly2/PAA/rhBMP-2/PAA]$_X$where X is the number of tetralayers. Poly2 is stable and positively charged under acidic deposition conditions, but undergoes hydrolytic degradation in a controlled manner when exposed to high pH aqueous solutions [38], resulting in first-order release from the LbL coating. In addition, the degradation of coatings reduces the area available for bacterial colonization, which may lead to the increased resistance to bacterial infection [44].

The laponite barrier layers, if necessary, were deposited atop the rhBMP-2 film using the spray LbL technique. The barrier layers consisted of a set of bilayers of cationic chitosan (Chi) or PDAC alternated with anionic laponite clay (Lap), indicated as $[Chi/Lap]_Y$or $[PDAC/Lap]_Y$where Y is the number of bilayers. During the assembly process, the kinetic time scale achieved with spray-LbL can lead to advantages over the control of interlayer diffusion and exchange processes that take place in the films with dip-LbL, resulting in minimal loss of therapeutics from underlying layers. This control ultimately leads to design of materials systems with distinct regimes and enhanced film stability. Furthermore, as the spray process is not diffusion limited, the assembly time for barrier layers is greatly reduced compared to the dip process, from 20 minutes to several seconds per bilayer.

The GS component were then introduced atop the rhBMP-2 film or the capped rhBMP-2 film as $[Poly1/PAA/GS/PAA]_Z$where Z is the number of tetralayers. A polycationic degradable poly(β-amino esters), Poly1, was alternated with anionic PAA and positively charged GS in the form of tetralayers. A top capping layer of $[Chi/Lap]_Y$or $[PDAC/Lap]_Y$was introduced as the final component, if necessary. The repeat units of the rhBMP-2 component, the laponite barrier layers, and the GS component are referred to as B_X, L_Y, and G_Z, respectively, and subscripted by the number of iterations.

3.2 Function of clay barrier layers

To establish the function of the laponite clay barrier in blocking diffusion of the underlying component, the effect of barrier films on tuning the release properties of small molecule GS was examined using a GS film architecture of $[Poly1/PAA/GS/PAA]_Z$. The GS films without and with barrier layers $[PDAC/Lap]_Y$are referred to as *no-barrier* GS film (G_Z) and *barrier* GS film (G_ZL_Y).

Before and after spray coating of GS LbL film with laponite barrier layers (schematic in Figure 2A), the surface morphology of the film was examined using atomic force microscopy (AFM). AFM measurements gave RMS roughness values of 1.3 ± 0.1 and 9.3 ± 1.0 nm for the *no-barrier* and *barrier* GS film, respectively. A noticeable difference in surface morphology was observed in the AFM topology images (Figure 2B); the *no-barrie*r film shows a smooth and homogeneous morphology, whereas the *barrier* GS film with outermost laponite layer displays a rougher and more granular morphology that is characteristic of laponite clay layer as previously observed [45]. The size of disc-shaped clay particles was found to be 43 ± 11 nm, approximately double the average diameter of a single platelet, suggesting that the deposited clay particles consist of 2–3 platelets [46, 47]. The AFM phase images suggest that near-complete surface coverage by clay particles was achieved. These results confirm that the laponite layers were successfully deposited on the top of the polymeric LbL film using the spray LbL technique.

To evaluate the barrier effect of the laponite clay component, the ^{3}H-GS loaded films were constructed with and without the spray-LbL barriers, and the release kinetics of a *barrier* GS film consisting of two capped GS films in sequence ($G_{30}L_{10}G_{30}L_{10}$) versus the *no-barrier* GS film with equivalent total numbers of drug-containing layers (G_{60}) were examined (Figure 3). Here we aimed to design an antibiotic delivery platform that could prevent any surviving bacteria from recolonizing the implant surface after revision surgery. A desired release profile is a rapid release of drug for the first few days to eliminate existing infection, followed by a controlled linear release for multiple weeks (6–8 weeks) to maintain a minimum inhibitory concentration sufficient to prevent further infection and biofilm formation on the implant [14, 48]. Two different representations of the release data are shown: Figure 3B shows the total GS released per cm^2 of film surface area, and Figure 3C shows the increment of GS release measured between each time point.

As can be seen in Figure 3, the implementation of barrier layers resulted in a substantial improvement in sustained release: approximately 50% reduction in bolus release at early times and a 10-fold increase in the relevant release timescale, $t_{70\%}$—the time for 70% of GS release from the films. The desired release profile was attained using only 60 tetralayers for the *barrier* GS system ($G_{30}L_{10}G_{30}L_{10}$) while 200 tetralayers were required in a previously described film release system [17]. The decrease in the number of GS tetralayers indicates significant reduction in the assembly time and cost. Note that if a larger bolus release upon implantation is necessary to treat an infection immediately following surgery, a film with no capping layers ($G_XL_YG_X$) or simply a film without barrier (G_X)would be more suitable. The release rate can also be tuned by using different molecular weight M_w of PAA or varying the number of tetralayers (Figures S1 and S2). That is to say, the release properties of our drug delivery system can be easily tailored for other specific applications.

For a further assessment of the barrier effect, the effective diffusion coefficients of gentamicin $D_{eff,GS}$ in the films with and without the laponite barrier were estimated from the release data and compared. Assuming that release occurs only along the direction perpendicular to the substrate, the $D_{eff,GS}$ in the film was roughly estimated using $D_{\text{eff, GS}}=\frac{L^2}{\tau_{\text{GS}}}$ where L represents the film thickness. The estimated value for $D_{eff,GS}$ in the laponite barrier is ~0.1 μm^2/day, which is three orders of magnitude smaller than in the GS tetralayer component (Table S1). The significant difference in $D_{eff,GS}$ supports that the laponite barrier is effective in modulating the release kinetics by physically hindering the diffusion of the molecules.

3.3 Characterization of the combination films: Growth and Release

A therapeutic coating suitable for primary implant surgery would exhibit staggered release of antibiotic followed by growth factor, whereas one for revision surgery should have a rapid release of an antibiotic for the first few days, followed by a sustained release for multiple weeks along with growth factor. While the release characteristics required for individual therapeutics would depend on the specific application, we fabricated and examined multi-component films containing rhBMP-2 and GS with and without the laponite barrier layers, referred to as *Barrier* composite ($B_XL_YG_Z$or $B_XL_YG_ZL_Y$) and *No-barrier* composite (B_XG_Z), with the aim of demonstrating that this system could be tuned for specific orthopedic applications involving infection treatment *and* bone regeneration.

First, film growth of a *barrier* composite film consisting of a capped rhBMP-2 film and a capped GS film in sequence ($B_{40}L_{15}G_{40}L_{15}$) was tracked to determine a successful construction of a composite film with the laponite barriers. The dip-LbL rhBMP-2 component grows linearly with the number of rhBMP-2 tetralayers (B_X), increasing at 640 ± 33 nm per tetralayer, followed by the spray-LbL barrier component, which also increases linearly at 27 ± 8.2 nm per bilayer (Figure 4A). The dip-LbL GS component, however, exhibits a delayed linear growth—an induction (delay) period for the first 10–15 tetralayers, followed by a period of linear growth. The observed induction period for the GS component when deposited on the laponite barrier layers is likely due to surface effects that influence the film buildup until complete surface coverage is achieved [49]. After the induction period, the thickness increase becomes linear, which is consistent with our previously reported findings [17]. The cross-sectional SEM image and EDS mapping of the *barrier* composite film in Figure 4B confirm the presence of a laponite clay interlayer that physically separates the underlying rhBMP-2 component and the top GS components, as well as a laponite capping layer atop the entire film.

Having demonstrated that the composite films can be built with excellent fidelity and consistent growth of the rhBMP-2 and GS drug components, the carrier properties of the composite films were evaluated by examining their drug loading and release kinetics. Figure 5 shows cumulative release profiles for the composite films including the *no-barrier* composite ($B_{80}G_{40}$), the *single-barrier* composite ($B_{80}L_{15}G_{40}$), and the *double-barrier* composite ($B_{80}L_{15}G_{40}L_{15}$). The total rhBMP-2 doses were 6.5 ± 0.23, 6.1 ± 0.57, 6.0 ± 0.50, and 7.0 ± 0.31 μg/cm^2 for the *no-barrier* composite, the *single-barrier* composite, the *double-barrier* composite, and the single-component control (B_{80}), respectively; these numbers are the same within experimental error, indicating consistent rhBMP-2 loading in all three composite films. The total GS doses were 730 ± 10, 550 ± 19, 540 ± 40, and 450 ± 24 μg/cm^2 for the *no-barrier* composite, the *single-barrier* composite, the *double-barrier* composite, and single-component control G_{40}, respectively. The differences in the GS loading for the composite films are attributed to an increased level of interlayer diffusion between the two components compared to the single-component film. The difference in the GS loading between the *barrier* and *no-barrier* composite films indicates that the interlayer diffusion of GS into the rhBMP-2 containing layers of the film was limited by the laponite interlayer barrier during the assembly process. The data in Figure 5B and 5C demonstrate that the presence of the laponite barrier layers as a regulator of GS release remains effective; a more bolus release is observed with the *single-barrier* composite film, $B_{80}L_{15}G_{40}$, in comparison to the *double-barrier* system, $B_{80}L_{15}G_{40}L_{15}$, that contains a laponite capping layer. The first film may be desirable for applications where a large bolus of anti-infective may be desired (e.g. a case of existing infection), followed by a slow release of rhBMP-2; whereas, the second case is relevant for more sustained release over extended periods (e.g. for prevention of infection).

Table 1 summarizes several relevant release timescales, including the time for 50, 70, and 99% of rhBMP-2 release from the composite films with and without barrier layers along with the single-component film of rhBMP-2 (B_{80}) as a control. The relevant timescales were determined by examining each sample data set that contributed to the averages and standard deviations in Figure 5.

Together Figure 5 and Table 1 show that there are significant differences in rhBMP-2 release kinetics for both composite films with and without the barrier compared to the single-component rhBMP-2 film. The release of rhBMP-2 from the composite films had two phases, as observed for the single-component rhBMP-2 film (Figure S6). The first phase is diffusion-controlled release whereas the second phase is controlled by film degradation. The rhBMP-2 released from the *no-barrier* composite $B_{80}G_{40}$ at a relatively constant rate of ~800 ng/cm^2/day for the first 4 days of release, which was then reduced to ~100 ng/cm^2/day until complete elution. A comparable amount of rhBMP-2 was incorporated and released from the barrier composite film. The rate of rhBMP-2 release in the first phase, however, is greatly reduced from ~800 ng/cm^2/day to ~300 ng/cm^2/day by implementing the laponite interlayer barrier, which suggests that the barrier physically blocks the interlayer diffusion of rhBMP-2.

The final rhBMP-2 release time $t_{99\%}$ of the composite films extends to over 33–55 days versus 19 days for the single-component film. An order of magnitude increase in $t_{70\%}$ for the *no-barrier* composite film $B_{80}G_{40}$ compared to the single-component rhBMP-2 film B_{80} suggests that the top GS component, composed of ionically-croosslinked and densely packed high molecular weight PAA, plays a role as a barrier for the underlying rhBMP-2 component. The comparison of $t_{50\%}$ values for the rhBMP-2 release from the *no-barrier* composite with the *barrier* composites indicates that the implementation of laponite barrier layers reduces the release rate of rhBMP-2 in early times, resulting in a lower local concentration of rhBMP-2 over a longer period of time as evidenced in Figure 5. For bone

regeneration, a long-term delivery of rhBMP-2 (> 30 days) at low local concentration is more favorable than a short-term delivery at an equivalent dose since the large dose of rhBMP-2 can lead to increased bone resorption and hematoma [50–52]. Furthermore, it is more desirable to release growth factors following sufficient time to eliminate or lower levels of infection in surrounding tissue. Both of these goals are facilitated by the introduction of barrier layers of laponite, yielding a multi-purpose implant coating which can potentially treat bacterial infection for multiple weeks as new bone is generated at the interface (Figure 5C).

While the ability to tune release properties of the LbL films for controlled delivery of multiple drugs is of great importance, evidence of the bioactivity of the films is essential for evaluating the film coating as a promising adjuvant therapy for total joint arthroplasty and other bone tissue engineering applications. To this end, we assessed (1) the antibacterial activity of the films against *S. aureus* and (2) the osteogenic efficacy to induce differentiation of pre-osteoblast cells. For the following *in vitro* tests, the *double-barrier* composite film ($B_{80}L_{15}G_{40}L_{15}$) was used as a representative of the *barrier* composite system since the rhBMP-2 release behavior of the *single-barrier* and *double-barrier* composite films are the same within experimental error (Figure 5).

3.4 In vitro antibacterial activity of films against S. aureus

A gram-positive *S. aureus*, an infecting pathogen responsible for about one third of surgical-site infections [53] and two thirds of chronic osteomyelitis clinical isolates, was chosen as the microorganism of interest in this study [54]. The efficacy of GS loaded on the LbL films against *S. aureus* was evaluated by exploring the activity of the LbL films directly as well as drug release solutions using (1) the Kirby-Bauer disk diffusion assay on a bacteria-coated agar plate and (2) a microdilution assay.

Kirby-Bauer disk diffusion assay provides qualitative information regarding the amount of GS that has diffused through agar by measuring the clear zone of inhibition (ZOI). The ZOI greater than 15 mm are generally regarded as a good predictor of effective treatment against *S. aureus* [55]. The LbL films tested for this assay include (i) GS film (G_{40}), (ii) *no-barrier* composite film ($B_{80}G_{40}$), and (iii) *barrier* composite film ($B_{80}L_{15}G_{40}L_{15}$). In all cases, the measured ZOI's were 25–26 mm, indicating the antibacterial efficacy of GS released from the LbL films against *S.aureus* (Figure 6).

In addition to the Kirby-Bauer assays, the ability to inhibit the growth of bacteria was determined via microdilution assay to confirm the antibacterial efficacy of the *barrier* composite film, $B_{80}L_{15}G_{40}L_{15}$. Figure 6B shows the response of the bacteria to dilutions of GS released from the films. The minimum inhibitory concentration (MIC) value of film release GS is found to lie between 0.25 to 0.50 μg/mL, which is consistent with the MIC value for the used strain (0.3 μg/mL). Together, these observations confirmed that the film assembly and release process have no adverse effects on the antibacterial activity of GS, and that the composite films are highly antimicrobial and effective against the common source of infection *S. aureus*.

3.5 In vitro rhBMP-2 activity assay

During bone regeneration and repair processes, the presence of an osteoinductive agent is necessary for promoting osteoblast differentiation. To determine the ability of our composite LbL coating to create a favorable bone-forming environment, we examined the effects of rhBMP-2 released from our LbL films on osteogenic differentiation and mineralization using pre-osteoblast MC3T3-E1 cells. MC3T3-E1 cells were seeded into 6-well tissue culture plates, and an rhBMP-2 containing film on a culture insert (transwell) was placed in

each well (Figure 7A). Cells and LbL coated substrates were exposed to differentiation media (growth medium supplemented with 10 mM β-glycerol phosphate and 50 mg/mL L-ascorbic acid). The extent of differentiation was then determined via Alizarin red (AR) staining and alkaline phosphatase (ALP) activity assays. ALP serves as an early marker of induction of bone differentiation, whereas AR staining is used to evaluate calcium-rich deposits formed upon maturation. Culture with uncoated substrates in differentiation medium served as a control.

Cells were cultured with different films—(i) single-component rhBMP-2 film (B_{80}), (ii) *no-barrier* composite film ($B_{80}G_{40}$), and (iii) *barrier* composite film ($B_{80}L_{15}G_{40}L_{15}$)—and assayed for mineralization via alizarin red at day 21. The visual inspection of cultures after Alizarin red staining showed the preserved activity of rhBMP-2 released from all three different films, compared to the control (Figure 7B). This observation also indicates that the top film component in the composite system—gentamicin and/or laponite barrier layers—have minimally adverse effects on the cell proliferation and differentiation. The ALP/AR signals observed for the individual laponite barrier component and GS component were statistically insignificant compared to the uncoated control in differentiation medium. The cell viability test results confirmed that there is no apparent cytotoxicity associated with the composite films at these concentrations (Figures S3 and S4).

To study the rhBMP-2 dose-dependent behavior of MC3T3-E1 cells, we then exposed the cells to different formulations released from the *barrier* composite film ($B_XL_{15}G_{40}L_{15}$) with varying numbers of rhBMP-2 tetralayers (X). The loading of rhBMP-2 in the composite film increased linearly with the number of layers as previously observed for the single-component rhBMP-2 film [18]; the total rhBMP-2 dose varied from 2.7 ± 0.31 μg/cm^2 for X = 40 to 8.5 ± 0.74 μg/cm^2 for X = 120. The ALP and AR signals for the $B_XL_{15}G_{40}L_{15}$ films with X = 40, 80, and 120 showed a dose-dependent effect of rhBMP-2 released from the composite film on bone differentiation (Figure 7C).

Having demonstrated that rhBMP-2 released from the composite films is highly effective in promoting osteogenic differentiation, we next sought to compare the bioactivity of rhBMP-2 over the course of the release study (up to 5 weeks) for different staged release formulations. The release sample was collected at each time point and tested via an ALP colorimetric assay as well as an ALP staining assay using NBT/ BCIP solution.

Compared to the single-component rhBMP-2 film (B_{80}), from which 90% of rhBMP-2 was eluted by 9 days, the composite films yielded more sustained release at a relatively constant rate, and the corresponding ALP responses confirm the trend (Figure 8). The ALP production of cells exposed to the composite films continued at a relatively constant rate over 4 and 5 or greater weeks, respectively, for the *no-barrier* ($B_{80}G_{40}$) and *barrier* films ($B_{80}L_{15}G_{40}$ or $B_{80}L_{15}G_{40}L_{15}$), while decreasing exponentially after a week for cells exposed to the single-component film (B_{80}). In addition, the visual inspection of temporal expression patterns revealed by ALP staining (Figure 8A) further supports that the laponite barrier has an impact on sustaining the release of rhBMP-2 from a composite film, providing a favorable release profile of rhBMP-2; the experiment ended at week 5, but it is apparent that the *barrier* composite film is still releasing at a relatively constant rate even at this time point, although the *no-barrier* composite film is beginning to taper in its release by week 5. Either composite films with or without barrier layers works well in term of osteogenic differentiation compared to the single-component control; in future work, *in vivo* studies will determine the best systems for osteogenesis.

4. Conclusion

This study demonstrated the ability to develop a multi-component LbL coating platform with highly tailored release profiles as an effective biomimetic implant surface that can deliver an antibiotic, gentamicin sulfate (GS), followed by a bone growth factor, rhBMP-2. For the fabrication of compartmentalized hybrid films with controlled and staged release profiles, we presented a new strategy—implementation of laponite clay barriers—that allows for a physical separation of multiple components by controlling interlayer diffusion. In a single-component GS multilayer film, the laponite clay barriers could effectively block interlayer diffusion, leading to 50% reduction in bolus doses and 10-fold increase in the release timescale ($t_{70\%}$). We presented a successful construction of composite films of rhBMP-2 and GS with and without laponite barrier layers and showed their high *in vitro* therapeutic efficacy over the course of the study. We found that the introduction of laponite barrier layers can enhance the temporal separation between release of the two drugs and extend release of the underlying rhBMP-2 growth factor, resulting in a more physiologically relevant dosing of rhBMP-2. Our findings highlight the characteristics of this new platform approach for multi-drug delivery, which can be easily fabricated, tuned, and translated to a variety of implants and devices.

Supplementary Material

Refer to Web version on PubMed Central for supplementary material.

Acknowledgments

This work was supported by the National Institutes of Health, National Institute of Aging (5R01AG029601-03). We thank Erik C. Dreaden, PhD for consultation on *in vitro* film studies, Sun Hwa Lee, PhD for assistance with SEM, and Ben Almquist, PhD, and Hyomin Lee for critical reading of the manuscript. The authors greatly appreciate the use of equipment available at the Institute for Soldier Nano-technologies (ISN), as well as the Robert Langer Laboratory for scintillation counting. We also acknowledge Pfizer Inc. for rhBMP-2.

References

1. Hammond PT. Polyelectrolyte multilayered nanoparticles: using nanolayers for controlled and targeted systemic release. Nanomed. 2012; 7:619–622.
2. Sundararaj SC, Thomas MV, Peyyala R, Dziubla TD, Puleo DA. Design of a multiple drug delivery system directed at periodontitis. Biomaterials. 2013
3. Chen F-M, Zhang M, Wu Z-F. Toward delivery of multiple growth factors in tissue engineering. Biomaterials. 2010; 31:6279–6308. [PubMed: 20493521]
4. Hammond PT. Form and function in multilayer assembly: new applications at the nanoscale. Adv Mater. 2004; 16:1271–1293.
5. DeMuth PC, Min Y, Huang B, Kramer JA, Miller AD, Barouch DH, et al. Polymer multilayer tattooing for enhanced DNA vaccination. Nat Mater. 2013; 12:367–376. [PubMed: 23353628]
6. Morton SW, Poon Z, Hammond PT. The architecture and biological performance of drug-loaded LbL nanoparticles. Biomaterials. 2013; 34:5328–5335. [PubMed: 23618629]
7. Poon Z, Chang D, Zhao X, Hammond PT. Layer-by-layer nanoparticles with a pH-sheddable layer for in vivo targeting of tumor hypoxia. ACS Nano. 2011; 5:4284–4292. [PubMed: 21513353]
8. Tang Z, Wang Y, Podsiadlo P, Kotov NA. Biomedical applications of layer-by-layer assembly: from biomimetics to tissue engineering. Adv Mater. 2006; 18:3203–3224.
9. Hong J, Shah NJ, Drake AC, DeMuth PC, Lee JB, Chen J, et al. Graphene multilayers as gates for multi-week sequential release of proteins from surfaces. ACS Nano. 2011; 6:81–88. [PubMed: 22176729]

10. Kim BS, Smith RC, Poon Z, Hammond PT. MAD (multiagent delivery) nanolayer: delivering multiple therapeutics from hierarchically assembled surface coatings. Langmuir. 2009; 25:14086–14092. [PubMed: 19630389]
11. Barthes J, Mertz D, Bach C, Metz-Boutigue M-Hln, Senger B, Voegel J-C, et al. Stretch-induced biodegradation of polyelectrolyte multilayer films for drug release. Langmuir. 2012; 28:13550–13554. [PubMed: 22957730]
12. Labek G, Thaler M, Janda W, Agreiter M, Stöckl B. Revision rates after total joint replacement: cumulative results from worldwide joint register datasets. J Bone Joint Surg. 2011; 93:293–297.
13. Hebert CK, Williams RE, Levy RS, Barrack RL. Cost of treating an infected total knee replacement. Clin Orthop. 1996; 331:140. [PubMed: 8895630]
14. Wenke JC, Guelcher SA. Dual delivery of an antibiotic and a growth factor addresses both the microbiological and biological challenges of contaminated bone fractures. Expert Opin Drug Deliv. 2011; 8:1555–1569. [PubMed: 22017669]
15. Nguyen A, Kim S, Maloney W, Wenke J, Yang Y. Effect of coadministration of vancomycin and BMP-2 on cocultured Staphylococcus aureus and W-20-17 mouse bone marrow stromal cells in vitro. Antimicrob Agents Chemother. 2012; 56:3776–3784. [PubMed: 22564844]
16. Goodman SB, Yao Z, Keeney M, Yang F. The future of biologic coatings for orthopaedic implants. Biomaterials. 2013; 34:3174–3183. [PubMed: 23391496]
17. Moskowitz JS, Blaisse MR, Samuel RE, Hsu HP, Harris MB, Martin SD, et al. The effectiveness of the controlled release of gentamicin from polyelectrolyte multilayers in the treatment of staphylococcus aureus infection in a rabbit bone model. Biomaterials. 2010; 31:6019–6030. [PubMed: 20488534]
18. Shah NJ, Macdonald ML, Beben YM, Padera RF, Samuel RE, Hammond PT. Tunable dual growth factor delivery from polyelectrolyte multilayer films. Biomaterials. 2011; 32:6183–6193. [PubMed: 21645919]
19. Shah NJ, Hong J, Hyder MN, Hammond PT. Osteophilic multilayer coatings for accelerated bone tissue growth. Adv Mater. 2012; 24:1445–1450. [PubMed: 22311551]
20. Shah NJ, Hyder MN, Moskowitz JS, Quadir MA, Morton SW, Seeherman HJ, et al. Surface-mediated bone tissue morphogenesis from tunable nanolayered implant coatings. Sci Transl Med. 2013; 5:191ra83.
21. Macdonald ML, Samuel RE, Shah NJ, Padera RF, Beben YM, Hammond PT. Tissue integration of growth factor-eluting layer-by-layer polyelectrolyte multilayer coated implants. Biomaterials. 2011; 32:1446–1453. [PubMed: 21084117]
22. Picart C, Mutterer J, Richert L, Luo Y, Prestwich G, Schaaf P, et al. Molecular basis for the explanation of the exponential growth of polyelectrolyte multilayers. Proc Natl Acad Sci. 2002; 99:12531–12535. [PubMed: 12237412]
23. Hammond PT. Engineering materials layer-by-layer: challenges and opportunities in multilayer assembly. AIChE Journal. 2011; 57:2928–2940.
24. Min Y, Hammond PT. Catechol-modified polyions in layer-by-layer assembly to enhance stability and sustain release of biomolecules: a bioinspired approach. Chem Mater. 2011; 23:5349–5357.
25. Wood KC, Chuang HF, Batten RD, Lynn DM, Hammond PT. Controlling interlayer diffusion to achieve sustained, multiagent delivery from layer-by-layer thin films. Proc Natl Acad Sci. 2006; 103:10207–10212. [PubMed: 16801543]
26. Garza JM, Schaaf P, Muller S, Ball V, Stoltz J-F, Voegel J-C, et al. Multicompartment films made of alternate polyelectrolyte multilayers of exponential and linear growth. Langmuir. 2004; 20:7298–7302. [PubMed: 15301518]
27. Mertz D, Vogt C, Hemmerlé J, Mutterer J, Ball V, Voegel J-C, et al. Mechanotransductive surfaces for reversible biocatalysis activation. Nat Mater. 2009; 8:731–735. [PubMed: 19668209]
28. Wang K, Ruan J, Song H, Zhang J, Wo Y, Guo S, et al. Biocompatibility of graphene oxide. Nanoscale Res Lett. 2011; 6:1–8.
29. Li Y, Maciel D, Tomás H, Rodrigues J, Ma H, Shi X. pH sensitive laponite/alginate hybrid hydrogels: swelling behaviour and release mechanism. Soft Matter. 2011; 7:6231–6238.

30. Gaharwar AK, Mihaila SM, Swami A, Patel A, Sant S, Reis RL, et al. Bioactive silicate nanoplatelets for osteogenic differentiation of human mesenchymal stem cells. Adv Mater. 2013; 25:3329–3336. [PubMed: 23670944]
31. Gaharwar AK, Schexnailder PJ, Kline BP, Schmidt G. Assessment of using laponite® cross-linked poly (ethylene oxide) for controlled cell adhesion and mineralization. Acta Biomater. 2011; 7:568–577. [PubMed: 20854941]
32. Viseras C, Aguzzi C, Cerezo P, Bedmar M. Biopolymer–clay nanocomposites for controlled drug delivery. Materials Science and Technology. 2008; 24:1020–1026.
33. Takahashi T, Yamada Y, Kataoka K, Nagasaki Y. Preparation of a novel PEG–clay hybrid as a DDS material: dispersion stability and sustained release profiles. J Control Release. 2005; 107:408–416. [PubMed: 16171884]
34. Cypes SH, Saltzman WM, Giannelis EP. Organosilicate-polymer drug delivery systems: controlled release and enhanced mechanical properties. J Control Release. 2003; 90:163–169. [PubMed: 12810299]
35. Joshi GV, Kevadiya BD, Patel HA, Bajaj HC, Jasra RV. Montmorillonite as a drug delivery system: intercalation and in vitro release of timolol maleate. Int J Pharm. 2009; 374:53–57. [PubMed: 19446759]
36. Liu L, Grunlan JC. Clay assisted dispersion of carbon nanotubes in conductive epoxy nanocomposites. Adv Funct Mater. 2007; 17:2343–2348.
37. Podsiadlo P, Kaushik AK, Arruda EM, Waas AM, Shim BS, Xu J, et al. Ultrastrong and stiff layered polymer nanocomposites. Science. 2007; 318:80–83. [PubMed: 17916728]
38. Lynn DM, Langer R. Degradable poly(beta-amino esters): synthesis, characterization, and self-assembly with plasmid DNA. J Am Chem Soc. 2000; 122:10761–10768.
39. Chuang HF, Smith RC, Hammond PT. Polyelectrolyte multilayers for tunable release of antibiotics. Biomacromolecules. 2008; 9:1660–1668. [PubMed: 18476743]
40. Gregory CA, Grady Gunn W, Peister A, Prockop DJ. An Alizarin red-based assay of mineralization by adherent cells in culture: comparison with cetylpyridinium chloride extraction. Anal Biochem. 2004; 329:77–84. [PubMed: 15136169]
41. Pashuck ET, Stevens MM. Designing regenerative biomaterial therapies for the clinic. Sci Transl Med. 2012; 4:160sr4. [PubMed: 23152328]
42. Andrews JM. Determination of minimum inhibitory concentrations. J Antimicrob Chemother. 2001; 48:5–16. [PubMed: 11420333]
43. Isefuku S, Joyner CJ, Simpson AHR. Gentamicin may have an adverse effect on osteogenesis. J Orthop Trauma. 2003; 17:212–216. [PubMed: 12621263]
44. Daghighi S, Sjollema J, van der Mei HC, Busscher HJ, Rochford ET. Infection resistance of degradable versus nondegradable biomaterials: an assessment of the potential mechanisms. Biomaterials. 2013; 34:8013–8017. [PubMed: 23915949]
45. Lutkenhaus JL, Olivetti EA, Verploegen EA, Cord BM, Sadoway DR, Hammond PT. Anisotropic structure and transport in self-assembled layered polymer-clay nanocomposites. Langmuir. 2007; 23:8515–8521. [PubMed: 17602505]
46. Fornes T, Paul D. Modeling properties of nylon 6/clay nanocomposites using composite theories. Polymer. 2003; 44:4993–5013.
47. Paul D, Robeson L. Polymer nanotechnology: nanocomposites. Polymer. 2008; 49:3187–3204.
48. Zilberman M, Elsner JJ. Antibiotic-eluting medical devices for various applications. J Control Release. 2008; 130:202–215. [PubMed: 18687500]
49. Macdonald M, Rodriguez NM, Smith R, Hammond PT. Release of a model protein from biodegradable self assembled films for surface delivery applications. J Control Release. 2008; 131:228–234. [PubMed: 18721835]
50. Jeon O, Song SJ, Yang HS, Bhang S-H, Kang S-W, Sung M, et al. Long-term delivery enhances in vivo osteogenic efficacy of bone morphogenetic protein-2 compared to short-term delivery. Biochem Biophys Res Commun. 2008; 369:774–780. [PubMed: 18313401]
51. Groeneveld E, Burger E. Bone morphogenetic proteins in human bone regeneration. Eur J Endocrinol. 2000; 142:9–21. [PubMed: 10633215]

52. Zara JN, Siu RK, Zhang X, Shen J, Ngo R, Lee M, et al. High doses of bone morphogenetic protein 2 induce structurally abnormal bone and inflammation in vivo. Tissue Eng Part A. 2011; 17:1389–1399. [PubMed: 21247344]

53. Wenzel RP, Bratzler D, Hunt D, van Rijen M, Bonten M, Wenzel R, et al. Minimizing surgical-site infections. N Engl J Med. 2010; 11:75–77. [PubMed: 20054050]

54. Soundrapandian C, Datta S, Sa B. Drug-eluting implants for osteomyelitis. Crit Rev Ther Drug Carrier Syst. 2007; 24:493–545. [PubMed: 18298388]

55. Darouiche RO, Mansouri MD, Zakarevicz D, AlSharif A, Landon GC. In vivo efficacy of antimicrobial-coated devices. J Bone Joint Surg. 2007; 89:792–797. [PubMed: 17403802]

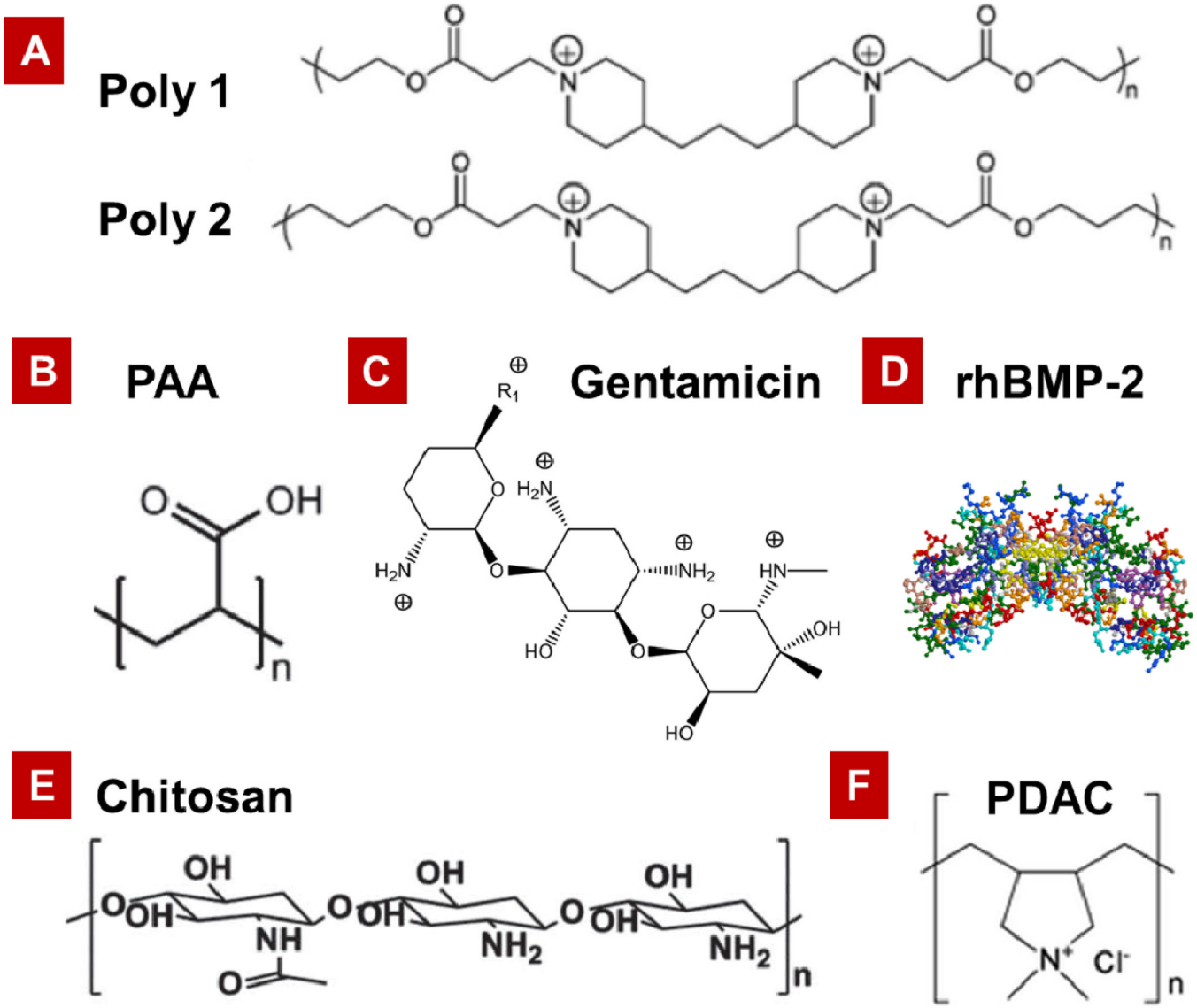

Figure 1.
Structure of (A) hydrolytically degradable Poly(β-amino esters), Poly1 and Poly2. (B) Poly(acrylic acid) (PAA). (C) Antibiotic, Gentamicin sulfate (GS). (D) Osteoinductive growth factor, rhBMP-2. (E) Chitosan (Chi). (F) Poly(diallyldimethylammonium chloride) (PDAC).

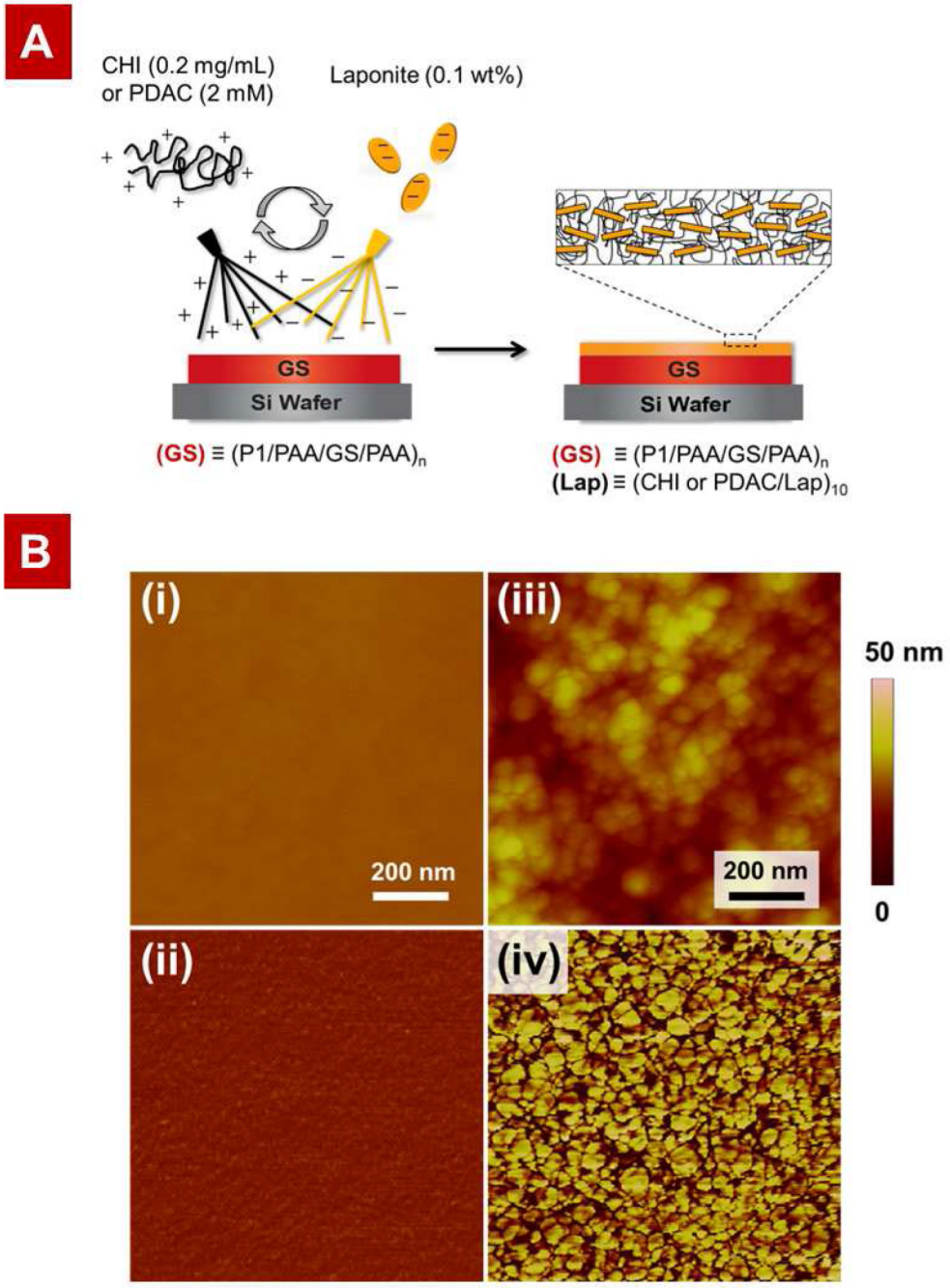

Figure 2.

Design and fabrication of the laponite barrier layers atop a GS-containing polymeric multilayer film: (A) Schematic of the spray layer-by-layer assembly of barrier layers on top of the GS dip-LbL films. (B) Atomic force microscopy (AFM) height and phase images of (i)–(ii) *no-barrier* GS film (G_{20}) and (iii)–(iv) *barrier* GS film ($G_{20}L_{10}$), respectively. In the phase images the stiff laponite particles appear bright while the soft polymer appears dark. Corresponding images confirm the successful deposition of barrier layers atop GS films.

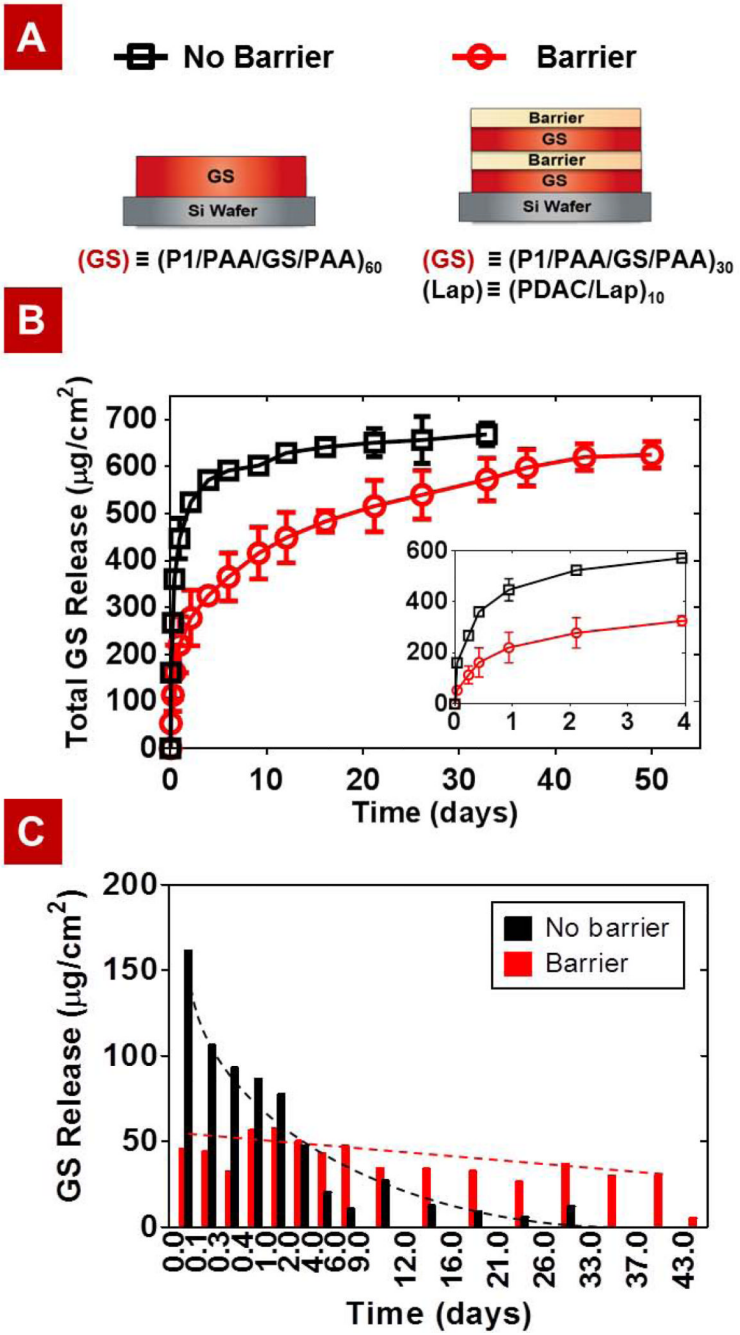

Figure 3.

Comparison of gentamicin (GS) release rate from GS films with and without barrier layers: (A) Schematic of the *No-barrier* GS film (G_{60}) and the *Barrier* GS film ($G_{30}L_{10}G_{30}L_{10}$). (B) Cumulative release profile of GS from G_{60} (□) and $G_{30}L_{10}G_{30}L_{10}$ (○). (C) The increment of GS release measured between each time point. The barrier layers control interlayer diffusion, which leads to a more sustained release. The dotted lines are drawn to aid the eye.

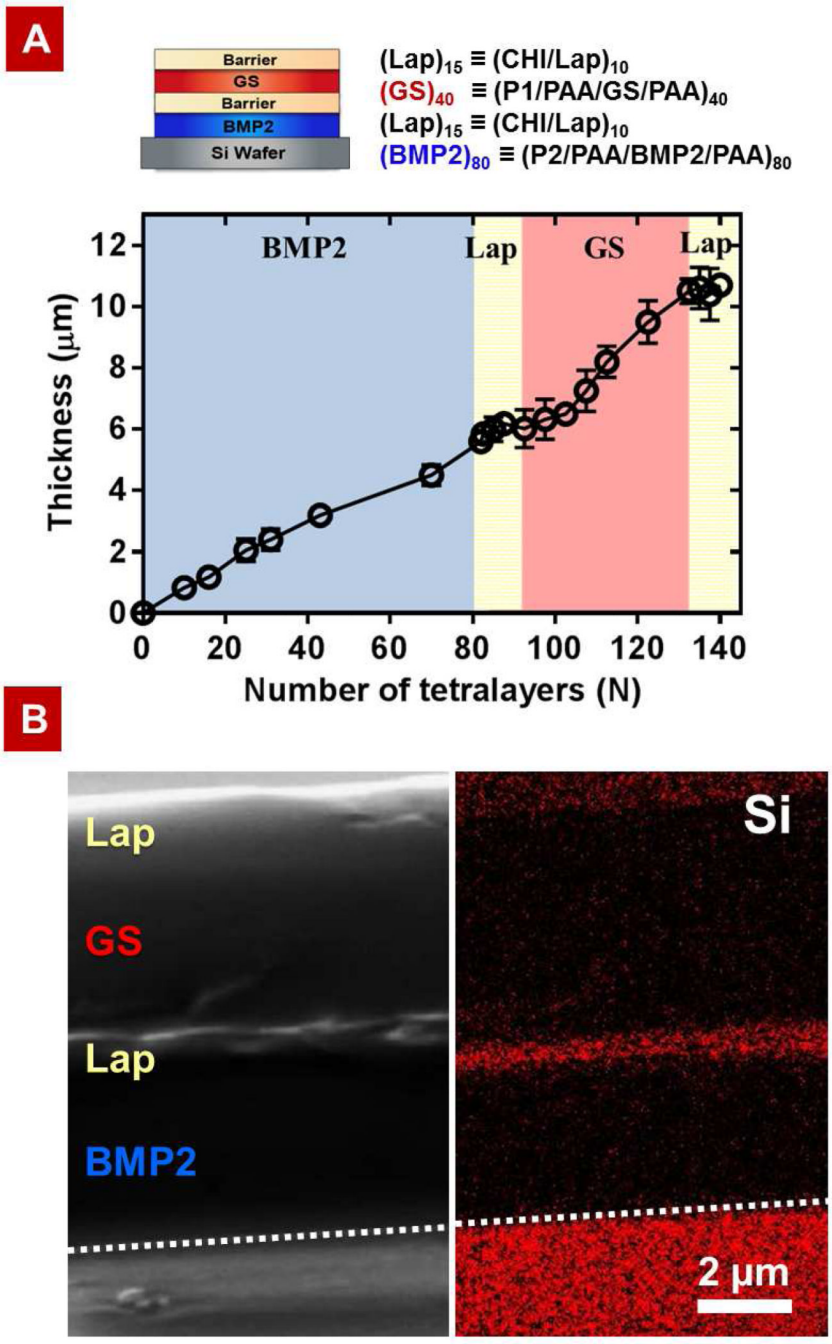

Figure 4.

Characteristics of multilayer properties during assembly: (A) Film architecture of electrostatically assembled composite films with barrier layers $B_{80}L_{15}G_{40}L_{15}$ and growth curve of the films as a function of tetralayer numbers *N* (a bilayer is counted as a ½ tetralayer). (B) Cross-sectional SEM image (left) of a composite film with laponite barrier layers $B_{40}L_{15}G_{40}L_{15}$ and its corresponding EDS mapping of element Si (right) confirm the compositional distribution of laponite in the film. The short dashed line indicates the position of the silicon substrate on which the LbL film was deposited.

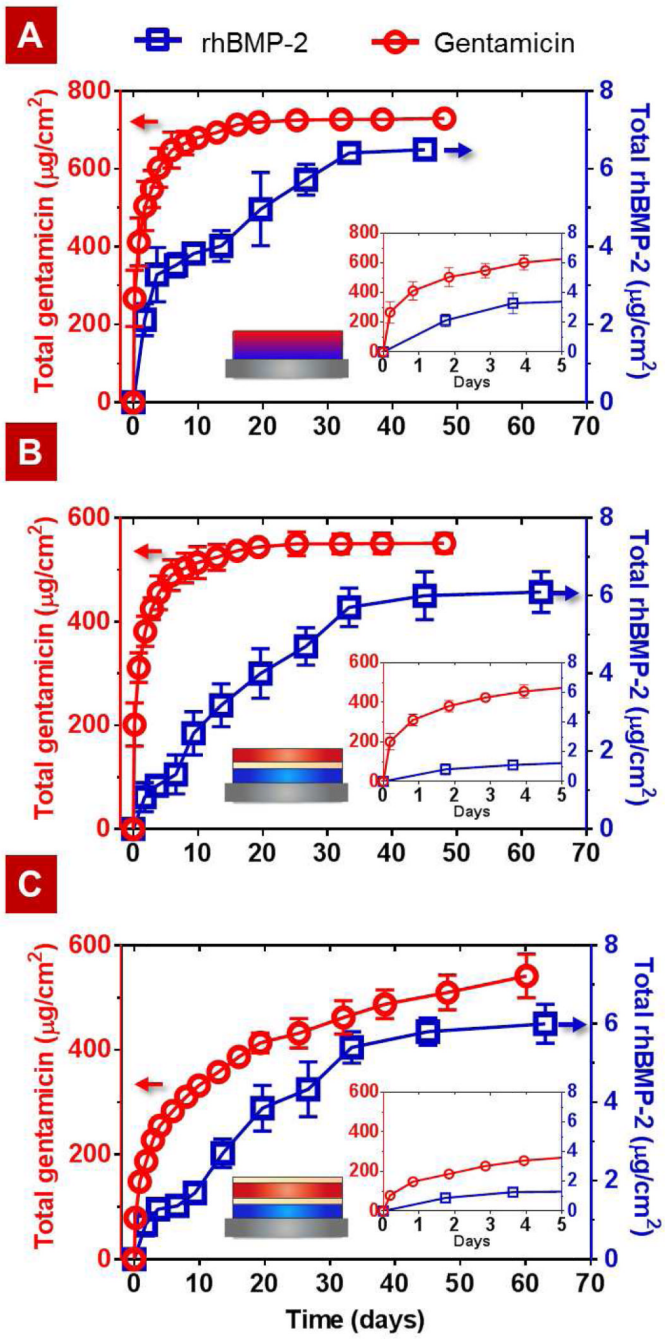

Figure 5.

Cumulative release profiles of GS (○) and rhBMP-2 (□) from the (A) *No-barrier* composite film $B_{80}G_{40}$, (B) *Single-barrier* composite film $B_{80}L_{15}G_{40}$, and (C) *Double-barrier* composite film $B_{80}L_{15}G_{40}L_{15}$. Inset shows a zoomed-in version of each figure for the initial 5 days.

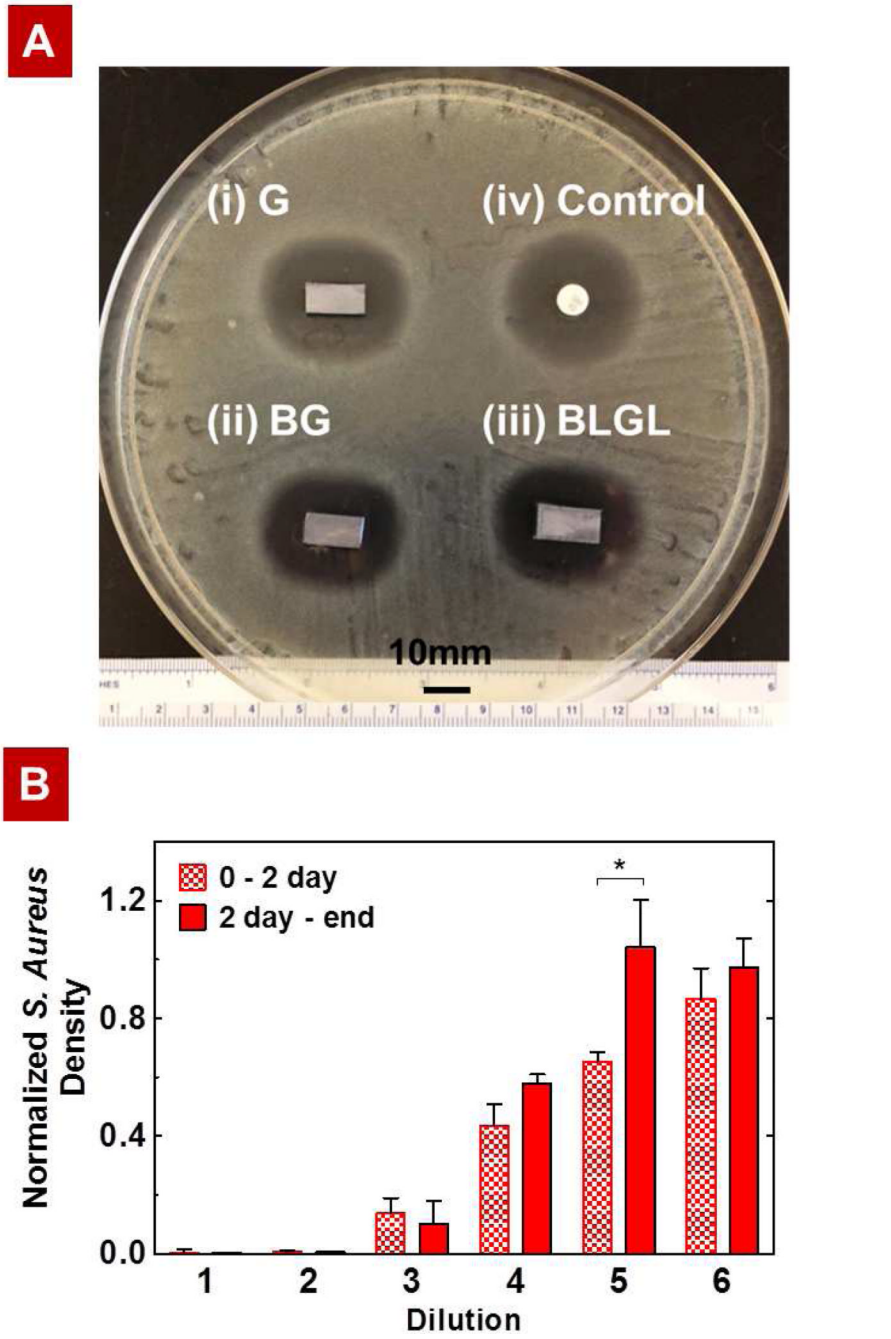

Figure 6.

(A) Comparison of the antibacterial activity of the LbL films with a commercially available BD Sensi-Disc via Kirby-Bauer assay. The silicon substrates coated with (i) G_{40}, (ii) $B_{80}G_{40}$, or (iii) $B_{80}L_{15}G_{40}L_{15}$ produced similar zones of inhibition (ZOI) of 25.6 mm against *S.aureus* (the ZOI is measured perpendicular to the long axis of the substrate). The Sensi-Disc standard with 10 μg of gentamicin, which produces a ZOI of 26.0 mm, served as control. (B) Normalized *S. Aureus* density upon exposure to dilutions of film release solutions (i.e., release from 0–2 days and from 2 days – end) from the barrier composite film $B_{80}L_{15}G_{40}L_{15}$ (dilution 1 = 1.0 ± 0.2 μg/mL). Each subsequent dilution is half the

concentration of the previous dilution. *$P < 0.05$, analysis of variance (ANOVA) with a Tukey post hoc test.

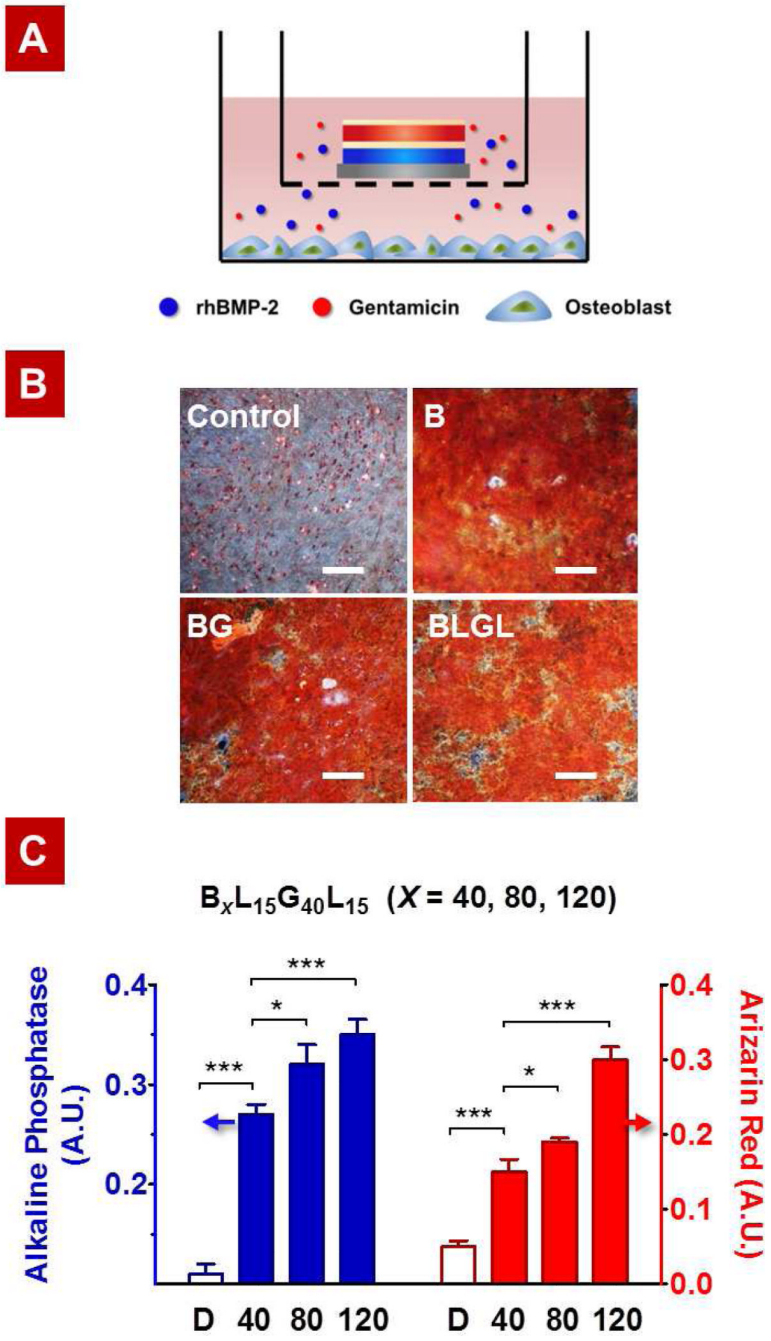

Figure 7.

Pre-osteoblast differentiation assay: (A) Representation of osteoblast culture for the evaluation of bioactivity of rhBMP-2 released from LbL films. (B) Visual inspection of cultures after Alizarin red staining confirms the preserved activity of rhBMP-2 released from B_{80} (B), $B_{80}G_{40}$ (BG), and $B_{80}L_{15}G_{40}L_{15}$ (BLGL) films. Culture with uncoated substrates in differentiation medium served as control. (C) Alkaline phosphatase (ALP) colorimetric assay at day 6 and Alizarin red assay at day 21 on cells differentiated with different release formulations as depicted ($B_XL_{15}G_{40}L_{15}$ where X = 40, 80, 120). ALP Assay demonstrates dose-dependent early activation of bone differentiation cascade at Day 5. After 21 days of culture, Alizarin Red quantification confirms the dose-dependent

presence of calcium deposits. Culture with uncoated substrates in differentiation medium served as control (D). *$P < 0.05$, **$P < 0.01$, ***$P < 0.001$, analysis of variance (ANOVA) with a Tukey post hoc test.

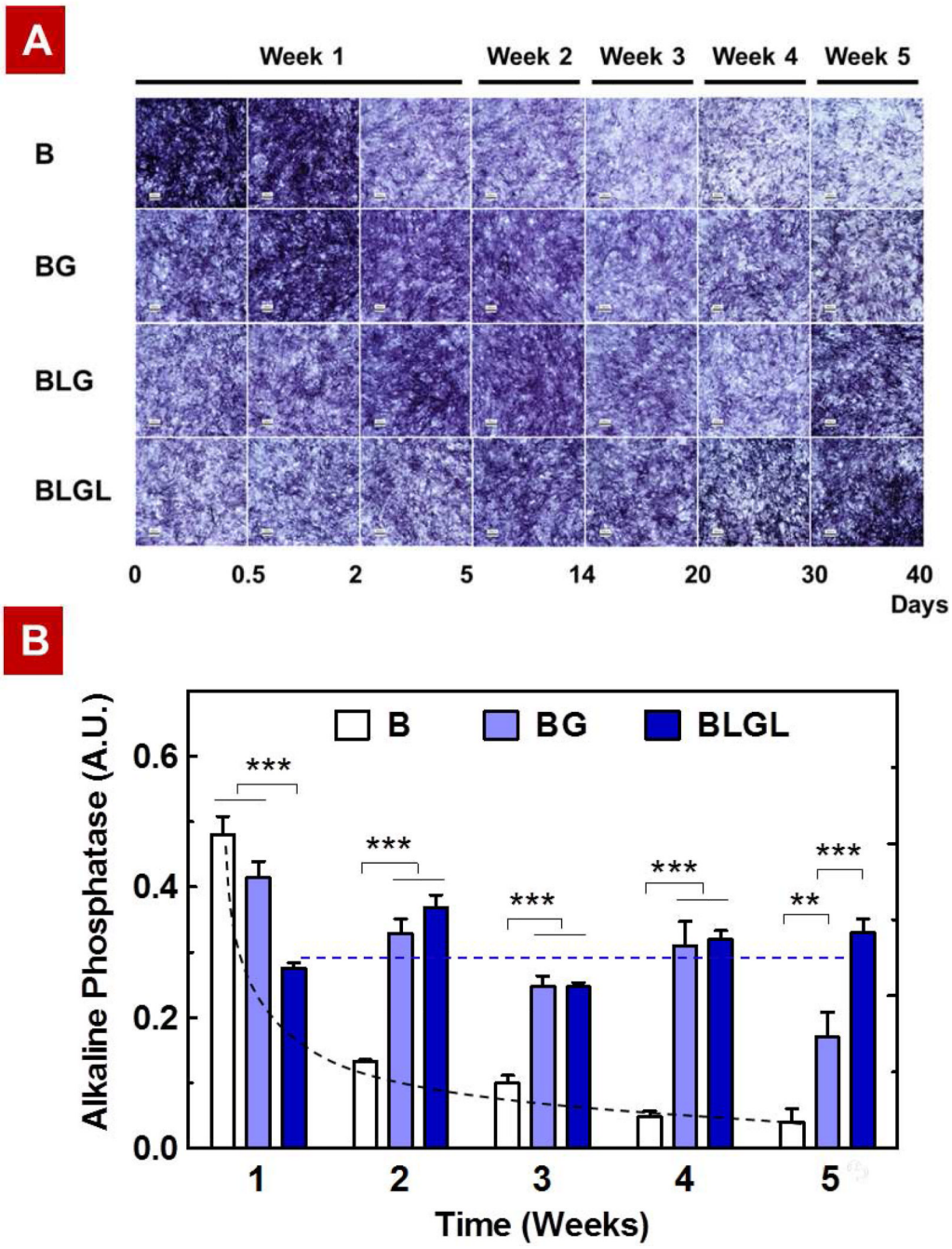

Figure 8.

Comparison of osteogenic efficacy of rhBMP-2 released from different delivery films—B_{80} (B), $B_{80}G_{40}$ (BG), $B_{80}L_{15}G_{40}$ (BLG), and $B_{80}L_{15}G_{40}L_{15}$ (BLGL)—(A) Visual inspection of temporal expression patterns for alkaline phosphatase (ALP) signals shows the sustained release of rhBMP-2 from composite films and the effect of barrier layers on modulating rhBMP-2 release. (B) ALP activity normalized to total protein confirms the observed release behaviors for different rhBMP-2 delivery films, and also demonstrates that the bioactivity of rhBMP-2 released from different films is preserved over the course of the study. Culture with uncoated substrates in differentiation medium served as control; its ALP activity was

0.04±0.01. The dotted lines are drawn by eye. *$P < 0.05$, **$P < 0.01$, ***$P < 0.001$, analysis of variance (ANOVA) with a Tukey post hoc test.

Table 1

Release kinetics of rhBMP-2 from different LbL films

	$t_{50\%}$ (days)	$t_{70\%}$ (days)	$t_{99\%}$ (days)
B_{80}	< 1	2	19
$B_{80}G_{40}$	3.5	17	33
$B_{80}L_{15}G_{40}$	13	22	47
$B_{80}L_{15}G_{40}L_{15}$	15	27	55